BSJ

REGULAR PAPER

Expression of tomato *SlTIP2;2* enhances the tolerance to salt stress in the transgenic *Arabidopsis* and interacts with target proteins

Shichao Xin · Guohong Yu · Linlin Sun ·
Xiaojing Qiang · Na Xu · Xianguo Cheng

Abstract Three independent transgenic *Arabidopsis* lines expressing *SlTIP2;2* from *Solanum lycopersicum* L. cv. Lichun under the control of its endogenous promoter were used to analyze the expression of *SlTIP2;2* and the salt stress tolerance under NaCl concentration gradient treatment. The expression patterns of *SlTIP2;2* were shown to be tissue-specific and NaCl dose-dependent under salt stress. *SlTIP2;2*-transformed *Arabidopsis* plants exhibited enhanced salt stress tolerance, and the physiological parameters suggested that *SlTIP2;2* has close links with the ion homeostasis and antioxidant enzymes activities in salt-stressed transgenic *Arabidopsis*. Moreover, *SlTIP2;2* expression significantly affected the Na^+ and K^+ fluxes from the root meristematic zones and resulted in remarkable changes in the morphology of the pith ray cells in the inflorescence stems of transgenic *Arabidopsis*. Based on the yeast growth assay, β-galactosidase activity testing and bimolecular fluorescence complementation, SlTIP1;1, SlTIP2;1 and an UDP-galactose transporter were confirmed to interact with SlTIP2;2, which may greatly broaden our understanding of the physiological functions of aquaporins.

S. Xin · G. Yu · X. Qiang · N. Xu · X. Cheng (✉)
Key Lab of Plant Nutrition and Fertilizers, Ministry of Agriculture, Institute of Agricultural Resources and Regional Planning, Chinese Academy of Agricultural Sciences, No. 12 South Street, Zhongguancun, Beijing 100081, China
e-mail: chengxianguo@caas.cn

L. Sun
College of Land and Environment, Shenyang Agricultural University, No.120 Dongling Road, Shenyang 110866, Liaoning, China

Introduction

Under natural conditions, plant growth and development are greatly affected by abiotic stresses, such as salinity, drought, and cold. The resistance of plants to such abiotic stresses relies heavily on the maintenance of their osmotic and ionic homeostasis, by means of the transportation and compartmentation of water and some solutes, which is realized via a combination of series of approaches (Chen and Polle 2010; Ruiz-Lozano et al. 2012). In these physiological processes, the transmembrane mobilization of water and/or small neutral solutes (urea, boric acid, and silicic acid) or gases (ammonia and carbon dioxide) is mainly conducted by aquaporins (AQPs) (Maurel et al. 2008). AQPs, also known as major intrinsic proteins (MIPs), are a class of small integral membrane proteins (approximately 23–34 kDa). Some AQPs can increase the hydraulic conductivity of the membrane by 10–20 times, and the transmembrane diffusion efficiency of water increases correspondingly (Obroucheva and Sin'kevich 2010).

A typical AQP monomer has six transmembrane α helixes, interrupted by three extra- and two intra-cellular loops, including two highly conserved asparagine-proline-alanine (NPA) motifs, and both C- and N-terminals facing the cytosol (Luu and Maurel 2005). Since the characterization of the first plant AQP in 1993 (Maurel et al. 1993), a large number of plant AQPs in a series of species have been identified. For instance, 36 AQPs have been reported in maize (Chaumont et al. 2001), 35 in *Arabidopsis*

_Springer

(Johanson et al. 2001), 33 in rice (Sakurai et al. 2005), 71 in cotton (Park et al. 2010) and 47 in tomato (Reuscher et al. 2013). AQPs are localized to different membranes, and perform different functions. They are categorized into five different clades on the basis of sequence homology: plasma membrane intrinsic proteins (PIPs), tonoplast intrinsic proteins (TIPs), nodulin 26-like intrinsic proteins (NIPs), small basic intrinsic proteins (SIPs), and the recently characterized X intrinsic proteins (XIPs) (Danielson and Johanson 2008; Johanson et al. 2001; Park et al. 2010). The members of the PIPs and TIPs are mainly targeted to the plasma membrane and the vacuolar membrane, respectively. The first identified member of NIPs, i.e. NOD26, is located on the peribacteroid membrane in soybean root nodules. NIPs reported in non-leguminous plants are localized on the plasma and intracellular membranes. SIPs are mostly located at the endoplasmic reticulum (ER) (Bansal and Sankararamakrishnan 2007; Ishikawa et al. 2005; Maurel 2007).

The functions of plant AQPs have been investigated by using inhibitors, heterologous coexpression in oocytes, detection of protein interactions in yeast mutants and overexpression in plants. The results of these studies indicate that AQP isoforms facilitate the mobilization of water, hydrogen peroxide, urea and some other solutes across the cell membranes of most living organisms (Carvajal et al. 1996; Hooijmaijers et al. 2012; Klebl et al. 2003; Maurel et al. 2008). Although generally considered as "always-open" channels, some AQPs can be regulated to cope with different environmental conditions. For instance, it has been reported that the hydrogen peroxide permeability of certain AQPs was enhanced through phosphorylation (Hooijmaijers et al. 2012). Several proteins in the AQP family can be phosphorylated, which is correlated with the regulation of their activities, leading to the adjustment of the absorption and transportation of water and/or some solutes, helping the plant adapt to changing environmental conditions (Ma et al. 2007; Maurel et al. 2008; Takano et al. 2006).

Membranes purified from wheat and tobacco showed that the tonoplast exhibits a dramatical higher (up to 100-fold) channel-mediated water permeability than the plasma membrane (Maurel et al. 1997; Niemietz and Tyerman 1997). This implicates the involvement of TIPs in buffering osmotic fluctuations under environmental stresses like salinity or drought. In the previous studies, the stress-induced regulations and distributions of TIPs were investigated by means of salt, mannitol, sorbitol or abscisic acid treatment. Exposure to salt slightly decreased the transcript abundance of certain TIPs in the root, which could prevent the deleterious effects from excessive salt intake (Boursiac et al. 2005). Osmotic stresses caused by mannitol, sorbitol or abscisic acid lead to a whole-plant up-

regulation of several TIPs (Vera-Estrella et al. 2004). In addition, the rapid and persistent osmotic stress-induced changes in the membrane allocation of TIPs indicate that the redistribution of TIPs is involved in the post translational control of TIP channel activities under stress conditions in plants (Vera-Estrella et al. 2004).

Tomato overexpressing a TIP gene *SlTIP2;2* showed significant increase in fruit yield, harvest index and plant mass relative to the control under both normal and water-stress conditions (Sade et al. 2009), suggesting that *SlTIP2;2* is a suitable candidate gene in improving the abiotic stress tolerance in plants. In the current study, three independent transgenic *Arabidopsis* lines carrying a *SlTIP2;2* transgene under the control of its endogenous promoter were obtained, and the expression patterns of *SlTIP2;2* in wild-type tomato and transgenic *Arabidopsis* exposed to salinity were analyzed. Further investigations regarding the role of *SlTIP2;2* in ion homeostasis in transgenic *Arabidopsis* were then conducted. Moreover, significant morphological changes were observed in the pith ray cells of transgenic *Arabidopsis* lines, and three novel interacting protein partners of *SlTIP2;2* were screened and confirmed, which in turn revealed some new probable roles of TIPs.

Materials and methods

Plant materials

Wild-type tomato (*Solanum lycopersicum* L. cv. Lichun) seeds were obtained from a local supplier and germinated under light for two days on moist filter paper, then transplanted into soil in a growth chamber under a 16 h light: 8 h dark cycle at 25 °C with 60 % relative humidity for four weeks. Next, the four-week-old wild-type tomato plants were used to study the effects of salt or drought stress on *SlTIP2;2* expression. In the salt stress assay, the tomato was exposed to a 200 mM NaCl concentration solution for 12 h. Meanwhile, the tomato in the drought treatment was not supplied with water for two weeks. For RNA preparation, representative root and shoot samples were taken from both the stressed and unstressed control groups. *Arabidopsis thaliana*, ecotype Columbia (Col-0), was kept at 22 °C in a soil-peat mixture for 10 h under light, and, and watered twice a week with tap water.

Isolation of *SlTIP2;2* target gene

Using an Easy Clone cDNA library construction kit (Dual systems Biotech, Zurich, Switzerland), full-length-enriched double stranded (ds) cDNA was synthesized from total RNA followed by subcloning into the library vector pPR3-

N. Based on the knowledge that AQPs are generally assembled as homotetramers in membranes (Verkman and Mitra 2000), an *Eutremahalophilum* AQP was used as the probe to find its orthologues in tomato. Split-ubiquitin yeast two-hybrid assay was conducted to screen the tomato cDNA library following the method described by Möckli et al. (2007). A full-length cDNA clone from tomato AQP (Accession no. JN798213) was obtained, and it is identical in AA sequences with the *SlTIP2;2* reported by Sade et al. (2009). The structure of *SlTIP2;2* gene in the tomato genome (Fig. 1a) was analyzed using the tomato gene model (ITAG release 2.3 SL2.40).

Construction of the plant expression vector and plant transformation

As shown in Fig. 1b, the open reading frame (ORF) sequence of *SlTIP2;2* and its putative promoter region (2-kb-long genomic DNA sequence upstream from the start codon of *SlTIP2;2*) were constructed into a modified binary vector pCAMBIA1304 using the primer pairs listed in Table S1. Then the constructed plant expression vector *SlTIP2;2*-pCAMBIA1304 was introduced into *Agrobacterium tumefaciens* strain C58. *Arabidopsis thaliana* ecotype Columbia (Col-0) plants were transformed following the floral dip method (Steven and Andrew 1998). The seeds collected were then selected on MS medium containing 40 mg L^{-1} hygromycin for three generations. The T3 generation of lines 1, 2 and 15 showed no segregation of hygromycin resistance, and were used in the following experiments.

Salt treatment

Four-week-old *Arabidopsis* plants, including three T3 transgenic lines and the wild-type control, were subjected to salt stress by irrigating solutions of different NaCl concentration (0, 50, 100, 150 and 250 mM). After 12 h of salt stress treatment, the roots and shoots of the three transgenic *Arabidopsis* plants were separately sampled to detect the relative transcript levels of *SlTIP2;2* under different NaCl concentration treatments. The three transgenic lines and the wild-type *Arabidopsis* under salt stress for four days were used to detect the whole-plant activity levels of superoxide dismutase (SOD), catalase (CAT) and peroxidase (POD). After two weeks of salt stress treatment, the plants were collected to determine the fresh weight, relative conductivity, water content, osmotic potential and content of ions.

Water content

The whole-plant water contents of the *SlTIP2;2*-transformed and wild-type *Arabidopsis* were determined. Fresh weight (FW) was immediately determined after sampling, then the plant materials were dried at 70 °C to a constant weight to record the dry weight (DW). Water content was calculated as [(FW − DW)/FW] × 100 %.

Osmotic potential

The *SlTIP2;2*-transformed and wild-type *Arabidopsis* after salt stress treatment were sampled and frozen at −80 °C for 5 h. All plant materials were cut into pieces and transformed into a syringe to extract the sap. The osmotic potential of the samples was measured using a osmotic pressure dew point meter (Wescor 5520, Logan, UT, USA) and calculated by the following equation: osmotic potential ψ_s (MPa) = –Ci × 0.008314 × (273 + T) × 10^{-3}, where Ci stands for instrument reading, and T for environment temperature.

Ion content

For ion content determination, the transgenic and wild-type *Arabidopsis* plants after two weeks of salt stress treatment were sampled, and washed with ultrapure water, and dried finally. Dry material of 100 mg was dissolved with mixed

Fig. 1 **a** The structure of *SlTIP2;2* gene in the tomato genome. **b** The promoter and open reading frame of *SlTIP2;2* were constructed into a plant expression vector
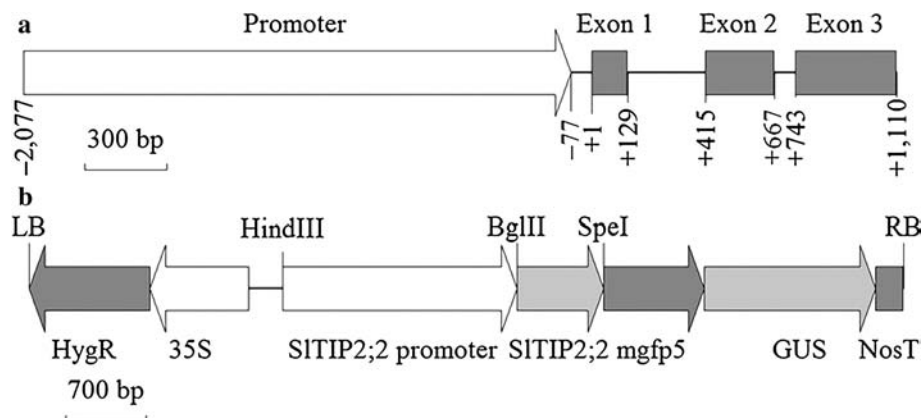
acid (nitric acid:sulfuric acid = 4:1) and heated at 180 °C until the solution becoming clear and transparent. The digested materials were diluted to 100 ml with ultrapure water, then the K^+ and Na^+ contents were measured using a flame photometer (410 Corning, Corning Science Products, Essex, UK).

Measurement of SOD, CAT and POD activities

The activities of SOD, CAT and POD were measured using a spectrophotometer (DR/2500, HACH, USA). About 500 mg of the plant materials after four days of salt stress treatment were used to extract the whole-plant SOD, CAT and POD, and a 5 ml extraction buffer containing 0.05 M phosphate buffer (pH 7.8) and 1 % polyvinyl pyrrolidone was added; the mixture was ground, then centrifuged at $10,000 \times g$ for 10 min at 4 °C; and the supernatant was collected to analyze the enzyme activities. Total POD activity was measured according to the method described by Polle et al. (1994). SOD and CAT activities were measured using SOD and CAT detection kits (S0102 and S0051, Beyotime, Shanghai, China), according to the manufacturer's instructions.

Relative conductivity

The sampled materials were cut into pieces and incubated in 25 ml of distilled water at room temperature for 12 h. The initial conductivity was measured ($\mu S\ cm^{-1}$, S1), as was the complete conductivity ($\mu S\ cm^{-1}$, S2) after boiling in a water bath for 15 min. The conductivity of the distilled water was also measured before (C1) and after (C2) being boiled in the water bath. Relative conductivity was calculated by the following equation: relative conductivity (%) = [(S1 − C1)/(S2 − C2)] × 100 %.

Ion flux assays

Five-day-old sterile-cultured seedlings of the three *SlTIP2;2* transgenic lines and wild-type *Arabidopsis* plants were used in the ion flux assays. Under normal conditions, the net fluxes of K^+ and Na^+ from the root epidermis in the meristematic (120 μm from the tip) zones of three transgenic lines and wild-type control were measured using a non-invasive micro-test technique, i.e. the scanning ion-selective electrode technique (SIET) using the SIET system (BIO-001B, Younger USA Sci. and Tech. Co., Amherst, MA, USA). Microelectrodes were filled with different selective liquid ion-exchange cocktails by Xuyue Science and Technology Cooperation Limited (Beijing, China) as described previously (Sun et al. 2009). During measurement, the electrodes were controlled by software to move between two positions close to the roots in a preset

excursion (30 μm from the root surface) at a programmable frequency in the range of 0.3–0.5 Hz. The ionic fluxes were calculated using Mage Flux developed by Xuyue Science and Technology Cooperation Limited (Beijing, China) (http://www.youngerusa.com/mageflux or http://xuyue.net/mageflux).

RNA extraction

The root and shoot tissues of the *Arabidopsis* and tomato plants were separately harvested into liquid nitrogen. According to the manufacturer's protocol, total RNA was isolated using the RNAiso Plus (TaKaRa Bio, Japan), and then determined using a DR/2500 spectrophotometer. RNA was stored at −80 °C. cDNA was prepared using AMV reverse transcriptase (Promega, Madison, WI), according to the manufacturer's protocol, and 2 μg of total RNA was used in each 20 μl reaction.

Semi-quantitative RT-PCR

To detect the expression of *SlTIP2;2* gene in wild-type tomato plants exposed to salt or drought stress, semi-quantitative RT-PCR was conducted using the primer pairs listed in Table S1. A 0.1-μl aliquot of cDNA prepared previously was used as the template in semi-quantitative RT-PCR, and Emerald Amp PCR Mastermix (Clontech, Mountain View, USA) comprising of all other required components was added. The PCR program for each primer pair was empirically adjusted. The resulting PCR products were then sequenced to confirm the specificity. *β-actin* and *Ef1α* were used as the constitutive standards. Agarose gels (1 %,w/v) were used to analyze the PCR products, and the nucleic acids were stained with ethidium bromide.

Quantitative RT-PCR

Quantitative RT-PCR techniques were used to detect the relative expression levels of *SlTIP2;2*. A 1-μl aliquot of the first strand cDNA was added to a 50-μl mixture containing 1× SYBR Premix Ex Taq (TaKaRa Bio, Japan) and 0.2 mM of each sense and antisense primers (Table S1) to initiate the PCR reaction. The primers used in the quantitative RT-PCR excluded the conserved domains to ensure high efficiency and specificity. Quantitative RT-PCR was performed on the Light Cycler system (Bio-Rad, Richmond, CA) under the PCR conditions at 98 °C for 2 min, and then cycling 40 cycles at 98 °C for 10 s, at 56 °C for 30 s, and at 68 °C for 1 min, and the resulting products were then sequenced. Three independent replicates were performed for each sample, and *β-actin* was used as the internal control. The relative expression levels of *SlTIP2;2* were then calculated using the $2^{-\Delta\Delta Ct}$ formula (Livak and

Schmittgen 2001). The mRNA fold differences were relative to those of 0 mM NaCl treated (treated with distilled water) samples used as a calibrator.

Analysis of inflorescence stem anatomy

Some sections of *Arabidopsis* inflorescence stems at a late growth stage (1–2 cm to the base) were fixed in FAA fixative (3.7 % v/v formaldehyde, 50 % ethanol, and 5 % acetic acid) overnight. Fixed samples were then treated as described by Gabe (1968). Sections (10 μm thick) were stained with 0.1 % fast green (Sigma, St. Louis, MO) in 95 % ethanol and examined under a light microscope.

Split-ubiquitin yeast two-hybrid assay

The split-ubiquitin yeast two-hybrid (SUY2H) system (Dual systems Biotech, Zurich, Switzerland) was used to screen the interacting protein partners of *SlTIP2;2* following the method described by Möckli et al. (2007). The poly (A+) mRNA extracted from wild-type tomato was transcribed into double-stranded cDNA comprising asymmetric *Sfi*I restriction sites, which allows the directional cloning of the cDNA library. The cDNA was amplified by PCR according to the manufacturer's instructions and ligated into the pPR3-N library vector. The ORF of *SlTIP2;2* was cloned into the pDHB1 bait vector, using the pair of *SlTIP2;2*-pDHB1 primers listed in Table S1 with *Sfi*I restriction site. The resulting constructs *SlTIP2;2*-pDHB1 and cDNA library were co-transformed into the yeast strain NMY51 using the yeast maker system (Clontech, Palo Alto, CA, USA), and the yeast cells were spread onto SD/–Leu–Trp plate to confirm the co-transformation efficiency and SD/–Leu/–Trp/–Ade/–His plate to detect the interactions, respectively, β-Galactosidase activity assay was conducted to confirm the interactions.

Bimolecular fluorescence complementation assay

In the yeast two-hybrid assay, three interacting protein partners of *SlTIP2;2* were obtained and numbered as 10#, 56#, and 114# (Table 1). To confirm these interactions in living cells, bimolecular fluorescence complementation (BiFC) assay was performed as described by Walter et al. (2004). The ORF of *SlTIP2;2* was inserted into the vector pUC-SPYNE, and 10#, 56# and 114# were constructed into the vector pUC-SPYCE, the corresponding primers for which are listed in Table S1. Therefore, the N-terminal fragment of YFP was fused to *SlTIP2;2*, and the C-terminal fragment of YFP was fused to 10#, 56# and 114#. For transient expression, the plasmids of interaction pairs were co-transformed into *Arabidopsis* protoplasts, mediated by polyethylene glycol (PEG), according to

Table 1 The partner proteins interacting with *SlTIP2;2* in yeast two-hybrid assay

Number	Accession number (nucleic acid)	Accession number (protein)	Amino acid residues	Definition
10#	AK246136	NP_001234103	250	Aquaporin TIP1;1-like protein
56#	AK325190	XP_004252567	327	Predicted: UDP-galactose transporter 2-like protein
114#	AK323926	XP_004252350	248	Predicted: aquaporin TIP2-1-like protein

Sheen's protocol (Yoo et al. 2007). Only *Arabidopsis* protoplasts co-expressing protein interaction pairs can emit yellow fluorescence signals. The construct pair of *SlTIP2;2*-nYFP with empty pUC-SPYCE vector was used as the negative control. *Arabidopsis* basic-leucine zipper bZIP63, which could form dimerization in the nucleus, was constructed into pUC-SPYNE and pUC-SPYCE, and the resulting constructs were co-transformed into *Arabidopsis* protoplasts as the positive control (Walter et al. 2004). After 16 h of incubation at 23 °C in the dark, the yellow fluorescence was observed using a LSM700 confocal laser microscope (Carl Zeiss AG, Oberkochen, Germany).

Results

Transcriptional regulation of *SlTIP2;2* in wild-type tomato and transgenic *Arabidopsis* plants

The effects of salt and drought stress on *SlTIP2;2* expression in wild-type tomato were studied using semi-quantitative RT-PCR (Fig. 2). The expression level of *SlTIP2;2* is responsive to salinity and drought. Down-regulation of *SlTIP2;2* expression occurred in the salt-stressed roots of wild-type tomato, while an increased transcript abundance of *SlTIP2;2* was observed in the shoots (Fig. 2a). Water deficit resulted in a transcriptional up-regulation of *SlTIP2;2* throughout the whole wild-type tomato plant, which was particularly evident in the shoots (Fig. 2b).

In the roots of salt-stressed T3 generation *SlTIP2;2*-transformed *Arabidopsis* plants, the expression of *SlTIP2;2* was reduced with the increasing NaCl concentration (Fig. 3a). However, the expression of *SlTIP2;2* was clearly up-regulated in the shoots after treatments with 100, 150 or 250 mM NaCl (Fig. 3b), and these data are consistent with
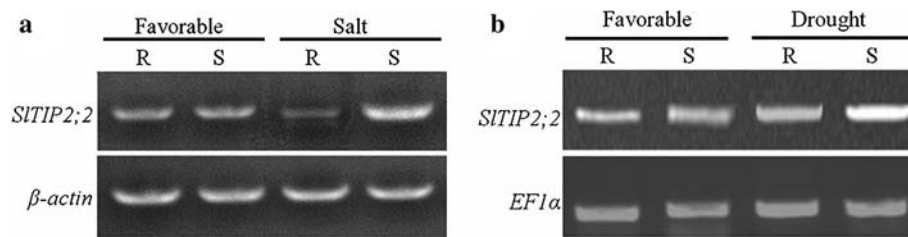
Fig. 2 The relative expressions of *SlTIP2;2* in wild-type tomato under salinity and drought. Six-week-old wild-type tomato plants were subjected to NaCl (200 mM) for 12 h or water deficit for two weeks, respectively. The roots and shoots were sampled separately for detecting the relative expression levels of *SlTIP2;2* by semi-quantitive

RT-PCR. R, the roots; S, the shoots. **a** Expression analysis of *SlTIP2;2* under salt stress. *β-actin* was used as the internal control. 28 PCR cycles were used for both *SlTIP2;2* and *β-actin*. **b** Expression analysis of *SlTIP2;2* under drought stress. *EF1α* was used as the internal control. 28 PCR cycles were used for both *SlTIP2;2* and *EF1α*
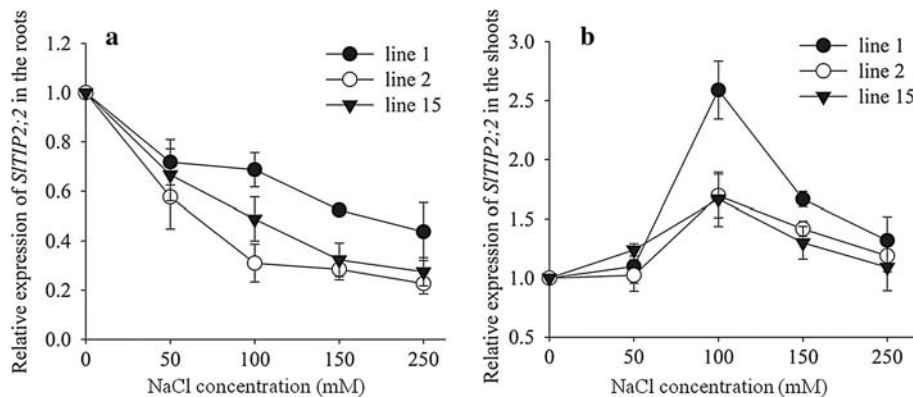
Fig. 3 Transcriptional regulation of *SlTIP2;2* in transgenic *Arabidopsis* under salt stress. **a** The relative expression levels of *SlTIP2;2* in the roots. **b** The relative expression levels of *SlTIP2;2* in the shoots. The roots and shoots of the three transgenic lines were sampled separately after 12 h of NaCl concentration gradient (0, 50, 100, 150, and 250 mM) treatment. The *y*-axis represents the relative fold

difference in mRNA level calculating using the $2^{-\Delta\Delta Ct}$ formula with *β-actin* as the internal control, and the mRNA fold difference was relative to that of 0 mM NaCl treated samples (treated with distilled water) as a calibrator. Data are mean ± SD of three replicates on one sample. Three biological experiments demonstrated similar results

the results of semi-quantitative PCR in salt-stressed wild-type tomato plants. In addition, the expression levels of *SlTIP2;2* varied in different NaCl concentration treatments. Higher NaCl concentration resulted in lower expression levels of *SlTIP2;2* in the roots (Fig. 3a). In the shoots (Fig. 3b), the maximum transcript abundances of *SlTIP2;2* were observed under 100 mM NaCl concentration treatment, then higher NaCl levels led to slight increases in the transcript abundance of *SlTIP2;2*.

### Effects of *SlTIP2;2* expression on salt stress tolerance in *Arabidopsis* plants

To investigate the exact roles of *SlTIP2;2*, several physiological parameters of the salt-stressed transgenic and wild-type *Arabidopsis* plants were determined, and are shown in Fig. 4. Osmotic potential, water content and fresh weight were inversely related to the increasing NaCl levels, and unstressed (0 mM NaCl treatment) transgenic and

wild-type *Arabidopsis* plants showed no significant differences. Under salt stress, the transgenic *Arabidopsis* plants maintained a slightly lower osmotic potential than the wild-type control (Fig. 4a). Meanwhile, the three transgenic lines showed significantly higher water content (Fig. 4b) and fresh weight (Fig. 4c) than the wild-type plants under high NaCl concentration (100, 150 and 250 mM) treatment.

As an important marker of salt tolerance in plants, the K^+/Na^+ ratio was determined, and data showed that the values decreased with increasing NaCl concentration (Fig. 4d). Under high NaCl concentration (100, 150 and 250 mM) treatment, the transgenic lines were able to maintain a higher K^+/Na^+ ratio than the wild-type control.

The activities of several antioxidant enzymes were also determined, and the results are shown in Fig. 4e–g. No significant differences in the SOD, CAT and POD activities were observed between the transgenic and wild-type lines under low NaCl levels (0 and 50 mM). But the three

Fig. 4 Several physiological parameters of the salt-stressed transgenic and wild-type *Arabidopsis* plants at the whole-plant level. Four-week-old *Arabidopsis* plants, including three *SlTIP2;2* transgenic lines (1, 2, and 15) and the wild-type control,were subjected to different NaCl concentration (0, 50,100,150 and 250 mM) treatments. **a** Osmotic potential. **b** Water content. **c** Fresh weight. **d** K^+/Na^+ ratio. **e** Activities of superoxide dismutase (SOD). **f** Activities of catalase (CAT). **g** Activities of peroxidase (POD). **h** Relative conductivity. Data are mean ± SD calculated from three replicates. *Asterisks* indicate significant difference between the wild-type control and the transgenic lines at $P < 0.05$ according to independent *t* tests. Three biological experiments were performed, which showed similar results
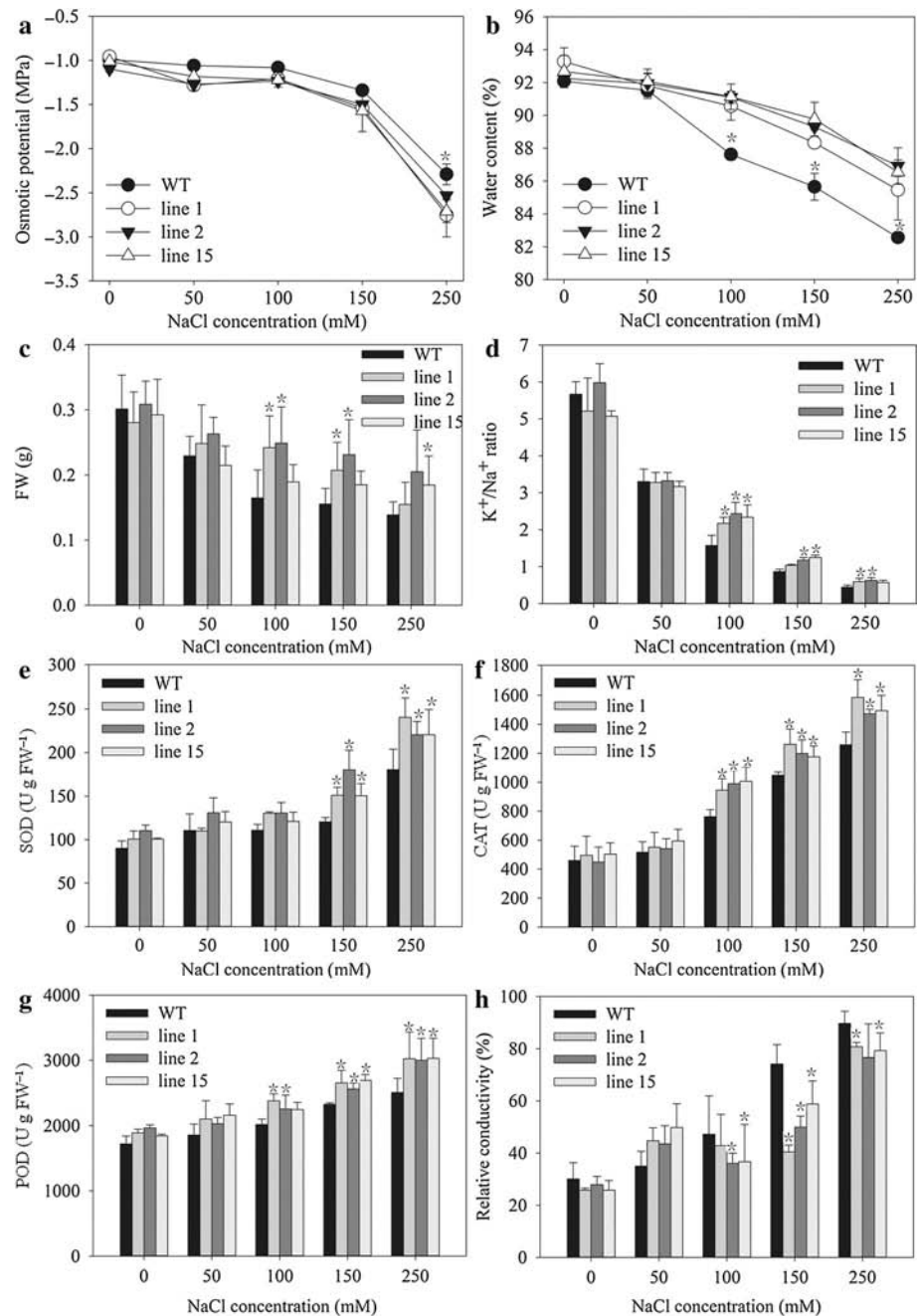
transgenic lines demonstrated higher SOD, CAT and POD activities than the wild-type control under high NaCl concentration treatments (100, 150 and 250 mM). Higher activities of antioxidant enzymes resulted in lower levels of stress-induced cell injury, which was reflected in the relative conductivity. Under high NaCl concentration (100, 150 and 250 mM) treatments, the wild-type control exhibited higher relative conductivity than the transgenic lines (Fig. 4h), indicating more serious membrane damage in wild-type *Arabidopsis* plants.

Effects of *SlTIP2;2* expression on Na^+ and K^+ fluxes in *Arabidopsis* plants

Under normal conditions, the Na^+ and K^+ fluxes from the root epidermis in the meristematic zones of transgenic and wild-type *Arabidopsis* lines were investigated, and are shown in Fig. 5. *SlTIP2;2*-transformation caused significant changes in Na^+ and K^+ fluxes. The Na^+ fluxes from the roots of transgenic and wild-type plants are effluxes (Fig. 5a), and the mean rates of the Na^+ effluxes in two of

the three transgenic lines were significantly lower than the wild-type control (Fig. 5b). The K$^+$ effluxes from the roots of the three transgenic lines were also significantly less than those of the wild-type plants (Fig. 5c, d).

Effects of SlTIP2;2 expression on inflorescence stem anatomy in Arabidopsis plants

Hanba et al. (2004) found that transgenic rice over-expressing an exogenous AQP gene exhibited anatomical changes. In the current study, the cross-sectional anatomy of Arabidopsis inflorescence stems showed that the pith ray cells (encircled by black frames) of SlTIP2;2 transgenic lines (Fig. 6a, c, e) were significantly different from those of the wild-type control (Fig. 6b, d, f). The inflorescence stems of the transgenic lines comprise fewer but larger pith ray cells than those of the wild-type Arabidopsis.
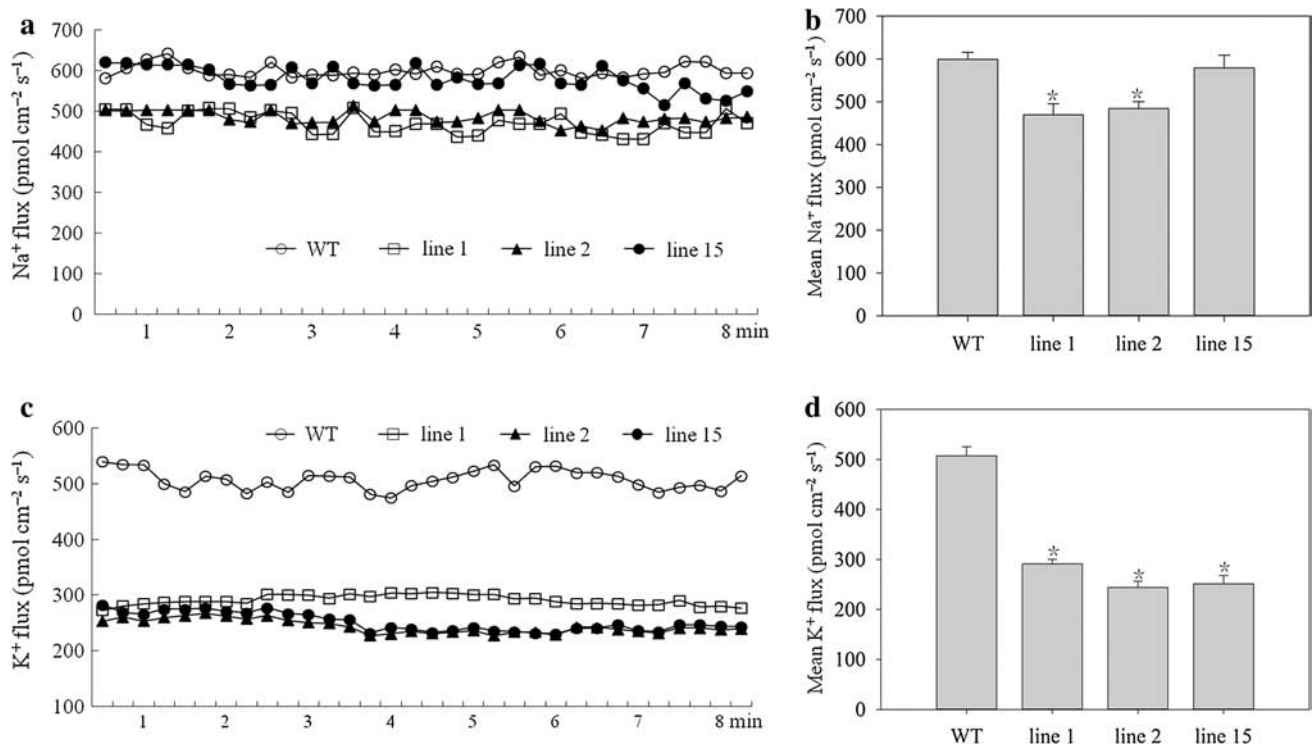
Identification of novel interacting protein partners of SlTIP2;2

Split-ubiquitin yeast two-hybrid assay was performed to find novel interacting protein partners of SlTIP2,2 in

tomato. As shown in Fig. 7a, several novel interactions of SlTIP2;2 were detected. These interacting protein partners are numbered as 10#, 56# and 114#, and listed in Table 1. In the subsequent β-galactosidase activity assay, some of the interacting proteins were proven to be false positives, such as 332# in Fig. 7a. Only yeast strains co-expressing protein interaction pairs can grow on the selected medium and turn blue in the β-galactosidase activity assay.

Bimolecular fluorescence complementation (BiFC) assays were then performed to further determine whether such interactions occur in vivo. When SlTIP2;2-nYFP was combined with 56#-cYFP, the yellow fluorescence signal was found as a spotty structure (Fig. 7b), confirming the interaction of SlTIP2;2 with the UDP-galactose transporter in plant cells. When SlTIP2;2-nYFP was combined with

Fig. 6 Cross-sectional anatomy of late growth stage Arabidopsis inflorescence stems (1–2 cm to the base). **a, c, e** SlTIP2;2-transformed Arabidopsis. **b, d, f** wild Wild-type Arabidopsis. pi, pith; xy, xylem; ph, phloem; pr, pith ray; ep, epidermis. Bar = 50 μm. The pith ray cells (encircled by black frames) of the transgenic Arabidopsis lines exhibited significant differences from those of the wild-type control


Fig. 5 Na$^+$ and K$^+$ fluxes (efflux positive) from the root epidermis in the meristematic zones of three transgenic lines (1, 2 and 15) and wild-type Arabidopsis plants under normal conditions. **a** Net Na$^+$ flux. **b** Mean rate of Na$^+$ flux. **c** Net K$^+$ flux. **d** Mean rate of K$^+$ flux. Na$^+$ and K$^+$ fluxes were measured immediately after the roots were sampled, and the measuring site was 120 μm from the root apex. Five biological experiments demonstrated similar results. Data are mean ± SD calculated from the values obtained during 8 min measurement. Independent t tests were conducted, and the asterisks indicate significant difference between the wild-type control and the transgenic lines at $P < 0.05$

J Plant Res
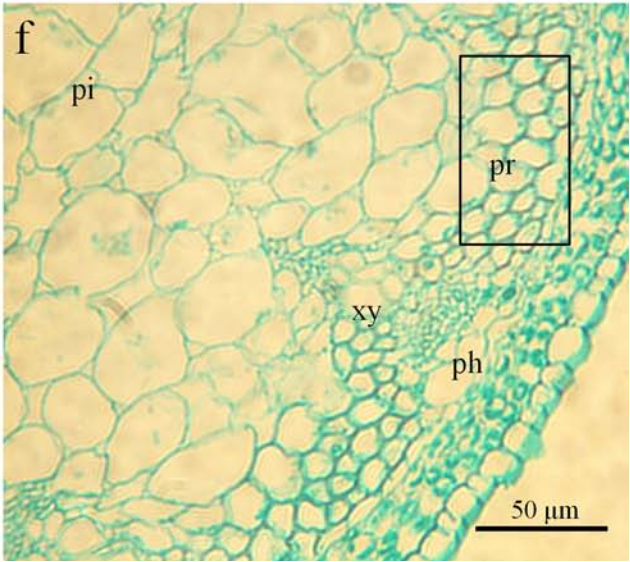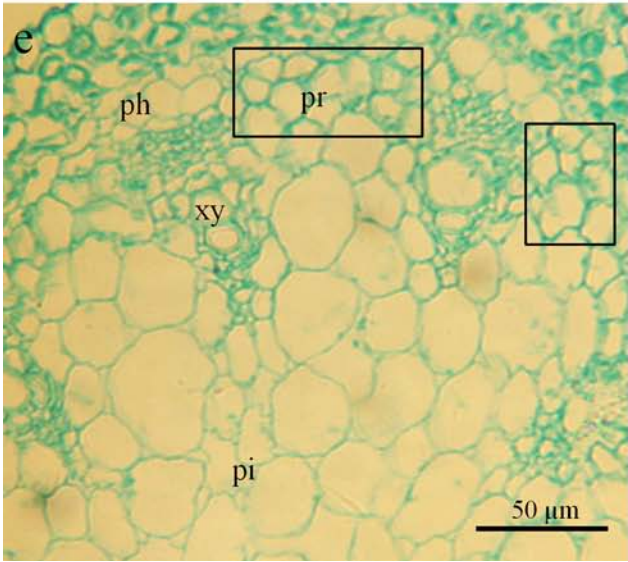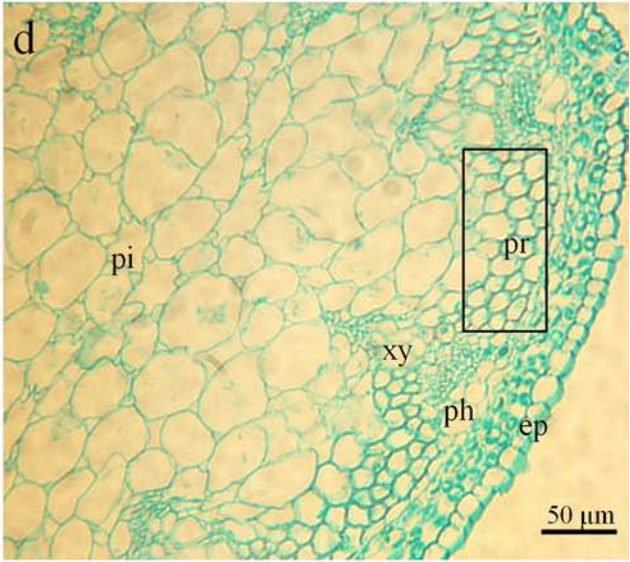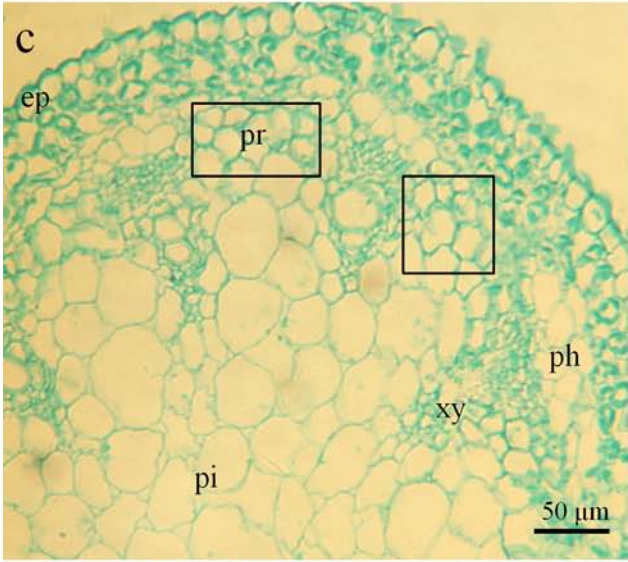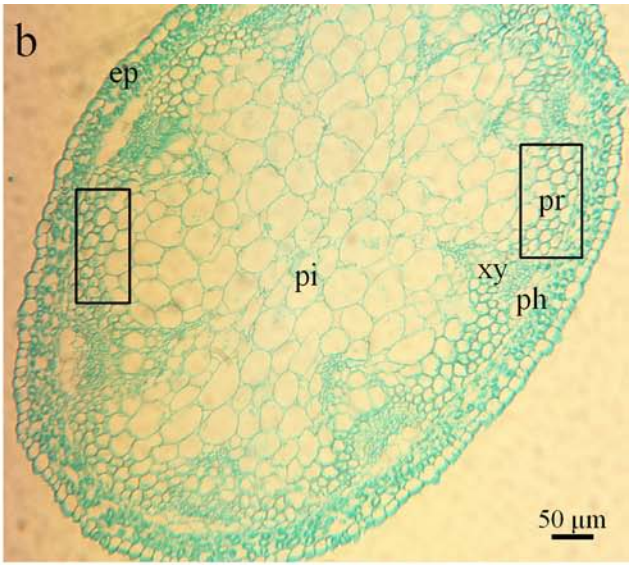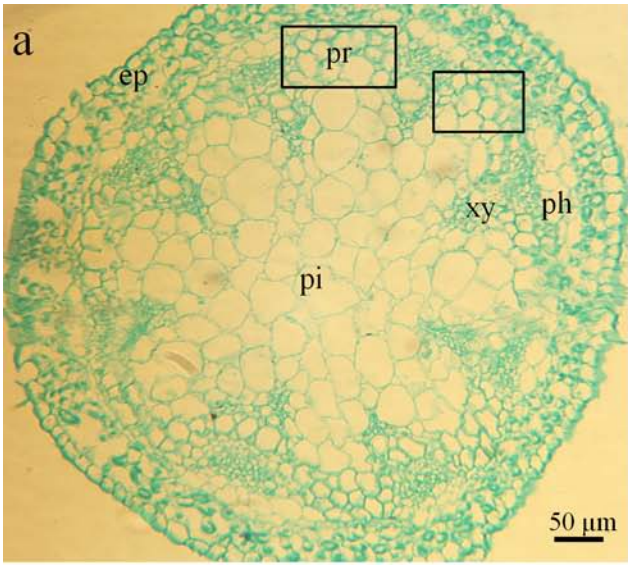
Fig. 7 Identification of the novel interacting protein partners of *SlTIP2;2*. **a** Split-ubiquitin yeast two-hybrid assay. The resulting constructs with empty pDHB1 bait vector or pPR3-N prey vector were co-transformed into yeast strain NMY51 as the negative control. The interactions were monitored by the growth of yeast on selective medium (SD/-Leu/-Trp/-Ade/-His) and the β-galactosidase activity assay. **b** Bimolecular fluorescence complementation (BiFC) assay in *Arabidopsis* protoplast. YFP fluorescence, bright field, chlorophyll and merged images are shown for each transformation combination. bZIP63 is a well-known transcription factor which can form dimerization in the nucleus. Hence, the construct pair of bZIP63-nYFP and bZIP63-cYFP fusions was used as the positive control. The construct pair of *SlTIP2;2*-nYFP and empty vector expressing cYFP was used as the negative control. *Bar* = 10 μm. The yeast two-hybrid and BiFC assays were carried out three times with similar results

🙋 Springer
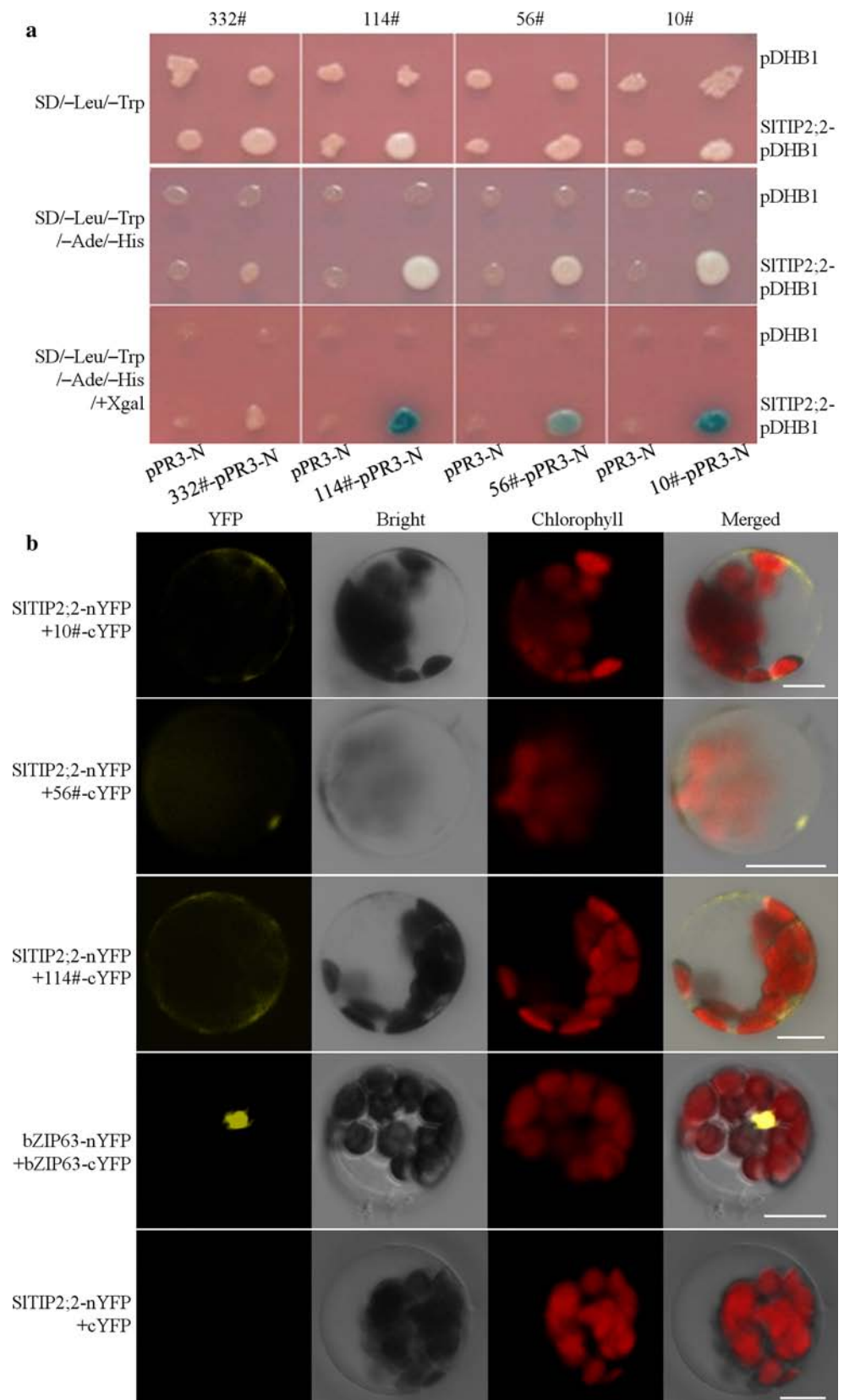
10#-cYFP or 114#-cYFP, the yellow fluorescence signal was visible in internal membranes and at the periphery of the *Arabidopsis* protoplasts (Fig. 7b), suggesting that *SlTIP2;2* could form heterotetramers in tomato. Mahdieh et al. (2008) found that interactions between some AQPs may lead to redistributions. To investigate whether or not *SlTIP2;2* demonstrate similar redistribution, BiFC assays by marking the plasma membrane and the vacuoles are now underway.

Discussions

Salt stress modulates expression of *SlTIP2;2*

Using computational approach, Sade et al. (2009) analyzed the expression patterns of *SlTIP2;2* and the results showed that expression of *SlTIP2;2* was enhanced in sixfold under various abiotic stresses. While the expression patterns of AQP genes in salt-stressed plants appear to be more complex. Uno et al. (1998) found that the transcript levels of three AQP genes vary among leaves and suspension-cultured cells under same salt stress conditions. In addition, the transcript levels of seven barley AQP genes responded differently to 100 mM NaCl treatment depending on the type of gene and plant tissue (Ligaba et al. 2011). In the current study, the expressions of *SlTIP2;2* in the roots of the wild-type tomato and transgenic *Arabidopsis* plants after 12 h of salt stress treatment were significantly down-regulated and inversely related to increasing NaCl concentrations (Figs. 2a, 3a), which is different from the results of the digital-expression computations performed by Sade et al. (2009). The down-regulation of *SlTIP2;2* expression in the roots could be interpreted by the purpose to reducing water efflux and preventing the deleterious effects of excessive salt loading. In the shoots, the transcript abundance of *SlTIP2;2* was increased by varying degrees under different NaCl concentration treatments. Overall, our work revealed the tissue-specific and NaCl dose-dependent regulation of *SlTIP2;2* expression.

Transgenic *Arabidopsis* plants expressing *SlTIP2;2* showed improved tolerance to salinity

Sade et al. (2009) proposed that *SlTIP2;2* overexpression improved tomato growth under salt stress by preventing the reduction of the tonoplast water permeability. Our results indicated that *SlTIP2;2*-transformed *Arabidopsis* lines were able to maintain a slightly lower osmotic potential (Fig. 4a) and significantly higher water content (Fig. 4b) than the wild-type control under salt stress. At the time of harvest the salt-stressed *SlTIP2;2* transgenic *Arabidopsis* lines

yielded significantly more fresh weight than the stressed wild-type control (Fig. 4c). These results suggested that *SlTIP2;2* expression enhanced the capability of transgenic *Arabidopsis* in osmotic regulation to resist excessive water efflux under salt stress.

In addition to excessive water efflux, plants exposed to salinity absorb more Na^+ and less K^+. Excessive Na^+ accumulation result in damages to plant cells, on the contrary, K^+ uptake and K^+ homeostasis are closely related with the ability to overcome salt-induced injury in plants (Ruiz-Lozano et al. 2012). Sade et al. (2009) proposed that *SlTIP2;2* probably does not participate in the mobilization of Na^+ ions. However, *SlTIP2;2*-transformed *Arabidopsis* lines were able to maintain a higher K^+/Na^+ ratio than the wild-type control under salt stress (Fig. 4d), suggesting a role for *SlTIP2;2* in Na^+ and/or K^+ homeostasis. Under normal conditions, Ma et al. (2014) found that the Na^+ and K^+ effluxes from the roots of the transgenic salt-tolerant tall fescue were lower than those of the wild-type control, and *SlTIP2;2* transgenic lines exhibited similar evidences in the current study (Fig. 5), suggesting that *SlTIP2;2* has some effects on Na^+ and K^+ fluxes in addition to the regulation of membrane water permeability. The molecular and cellular mechanism of the involvement of *SlTIP2;2* in ion fluxes remains unclear, and this may be due to the tight links between water and ion transport during cell turgor regulation.

Environmental stresses trigger generation of excessive reactive oxygen species (ROS), resulting in membrane dysfunction and cell death (Jiang and Zhang 2002). Antioxidant enzymes play a key role in protecting plants from excessive ROS (Ruiz-Lozano et al. 2012). Our results showed that *SlTIP2;2* expression enhanced the activities of SOD, CAT and POD in transgenic *Arabidopsis* under high NaCl concentration treatment (Fig. 4e–g). Hu et al. (2012) reported that overexpression of *TaAQP8* increased SOD, CAT and POD activities by enhancing the expressions of *NtSOD*, *NtCAT* and *NtPOD* in tobacco. Whether or not *SlTIP2;2* expression has similar impacts on the expressions of SOD, CAT and POD genes in *Arabidopsis* requires further investigations. Attributed to the higher activities of antioxidant enzymes, excessive reactive oxygen species (ROS) induced by salt overloading caused less cell injury in the three transgenic lines than the wild-type control (Fig. 4h). These results signified that *SlTIP2;2* transgenic lines were more vigorous than the wild-type control under salt stress.

Relationship between the anatomical changes in inflorescence stems and *SlTIP2;2* expression

Some TIPs are involved in plant cell expansion. For instance, the *Arabidopsis* AtTIP1;1 has a strong link with

cell enlargement and differentiation (Ludevid et al. 1992), which may be due to its complex roles in the accumulation of various sugars, organic acids and starch (Ma et al. 2004). In the current study, *SlTIP2;2*-transformed *Arabidopsis* exhibited significant anatomical changes in the pith ray cells of inflorescence stems, suggesting that *SlTIP2;2* may be involved in plant cell expansion as well. It may also be possible that the anatomical changes in *SlTIP2;2*-transformed *Arabidopsis* were simply the results of plant acclimation to some physiological changes, as described by Kawase et al. (2013). If *SlTIP2;2* changes the growth of *Arabidopsis*,the anatomy of the inflorescence stems would change accordingly.

Novel interactions of *SlTIP2;2*

In maize, heterotetramers formed by PIP1s with PIP2s lead to a promotion of water permeability and the relocalization of PIP1s to the plasma membrane (Zelazny et al. 2007). And the interaction of NtAQP1 with NtPIP2;1 is crucial for increasing CO_2 membrane conductance (Otto et al. 2010). The interactions among TIP isoforms have not been well studied yet. Murozuka et al. (2013) found that *Arabidopsis* tonoplast intrinsic proteins AtTIP1;2, AtTIP2;1 and At-TIP3;1 could interact with each other when heterologously co-expressed in yeast, which should be further confirmed in plant cells. In the current work, for the first time, we obtained three novel interacting protein partners of *SlTIP2;2*, and two of which are SITIP1;1 and SITIP2;1. Presently, we can not define the specific subcellular localizations and the exact roles of these interactions. In plant cells, endoplasmic reticulum (ER) is the only organelle equipped with TIP1s as well as TIP2s (Maurel et al. 2008), so the interaction of *SlTIP2;2* with SlTIP1;1 is supposed to occur on the ER. In wild-type tomato, *SlTIP2;2* was mainly expressed in the leaves, roots and flowers; *SlTIP2;1* was preferentially expressed in the young leaves and roots; while *SlTIP1;1* was only expressed in the flowers (Reuscher et al. 2013). These results suggest that the interaction of *SlTIP2;2* with SlTIP1;1 could only occur in the flowers, while the interaction of *SlTIP2;2* with *SlTIP2;1* could occur in the shoots, roots and flowers. Recent studies have shown that the expressions of some TIP isoforms are closely co-regulated to cope with various environmental stresses (Alexandersson et al. 2010), and interactions among TIPs in yeast were shown to be related to post-translational modifications, which may affect the channeling capacity of the TIPs (Murozuka et al. 2013). These results implicate the involvements of the interactions of *SlTIP2;2* with SlTIP1;1 and *SlTIP2;1* in regulating membrane permeability in adapting to changing environmental conditions.

Another interacting protein partner of *SlTIP2;2* is a putative UDP-galactose transporter and such interactions have not yet been reported. UDP-galactose is synthesized in the cytosol, and serves as the galactose donor in the biosynthesis of glycoproteins and glycolipids in the ER lumen. Reyes et al. (2006) found that an *Arabidopsis* UDP-galactose transporter is located on the ER, and functions in transporting UDP-galactose into the ER lumen. These results suggest that the interaction of *SlTIP2;2* with the UDP-galactose transporter may occur on the ER, and *SlTIP2;2* may also be involved in the trafficking of UDP-galactose. It may be an essential manner for *SlTIP2;2* to interact with other TIPs and the UDP-galactose transporter to function properly in some physiological processes. More investigations are now underway to reveal the specific subcellular localizations of these interactions, and these data encourage further studies on the functions of these interactions in plants.

Conclusions

The expression patterns of *SlTIP2;2* were shown to be tissue-specific and NaCl dose-dependent under salt stress. *SlTIP2;2* expression enhanced the salt stress tolerance in transgenic *Arabidopsis*. By measuring the K^+/Na^+ ratio and the ion fluxes, we found that *SlTIP2;2* may have a role in ion homeostasis. In addition, *SlTIP2;2* expression resulted in significant anatomical changes in the inflorescence stems of transgenic *Arabidopsis*. Moreover, three novel interacting protein partners of *SlTIP2;2* were screened and confirmed in vivo, and the specific physiological functions of these interactions are currently still under investigation.

References

Alexandersson E, Danielson JÅ, Råde J, Moparthi VK, Fontes M, Kjellbom P, Johanson U (2010) Transcriptional regulation of aquaporins in accessions of *Arabidopsis* in response to drought stress. Plant J 61:650–660
Bansal A, Sankararamakrishnan R (2007) Homology modeling of major intrinsic proteins in rice, maize and *Arabidopsis*: comparative analysis of transmembrane helix association and aromatic/arginine selectivity filters. BMC Struct Biol 7:27
Boursiac Y, Chen S, Luu DT, Sorieul M, van den Dries N, Maurel C (2005) Early effects of salinity on water transport in *Arabidopsis* roots. Molecular and cellular features of aquaporin expression. Plant Physiol 139:790–805

Carvajal M, Cooke DT, Clarkson DT (1996) Responses of wheat plants to nutrient deprivation may involve the regulation of water-channel function. Planta 199:372–381

Chaumont F, Barrieu F, Wojcik E, Chrispeels MJ, Jung R (2001) Aquaporins constitute a large and highly divergent protein family in maize. Plant Physiol 125:1206–1215

Chen S, Polle A (2010) Salinity tolerance of Populus. Plant Biol 12:317–333

Danielson JÅ, Johanson U (2008) Unexpected complexity of the aquaporin gene family in the moss Physcomitrella patens. BMC Plant Biol 8:45

Gabe M (1968) Techniques histologiques. Masson et Cie, Paris, pp 67–162

Hanba YT, Shibasaka M, Hayashi Y, Hayakawa T, Kasamo K, Terashima I, Katsuhara M (2004) Overexpression of the barley aquaporin HvPIP2;1 increases internal CO_2 conductance and CO_2 assimilation in the leaves of transgenic rice plants. Plant Cell Physiol 45:521–529

Hooijmaijers C, Rhee JY, Kwak KJ, Chung GC, Horie T, Katsuhara M, Kang H (2012) Hydrogen peroxide permeability of plasma membrane aquaporins of Arabidopsis thaliana. J Plant Res 125:147–153

Hu W, Yuan Q, Wang Y, Cai R, Deng X, Wang J, Zhou S, Chen M, Chen L, Huang C, Ma Z, Yang G, He G (2012) Overexpression of a wheat aquaporin gene, TaAQP8, enhances salt stress tolerance in transgenic tobacco. Plant Cell Physiol 53:2127–2141

Ishikawa F, Suga S, Uemura T, Sato MH, Maeshima M (2005) Novel type aquaporins SIPs are mainly localized to the EP membrane and show cell-specific expression in Arabidopsis thaliana. FEBS Lett 579:5814–5820

Jiang M, Zhang J (2002) Water stress-induced abscisic acid accumulation triggers the increased generation of reactive oxygen species and up-regulates the activities of antioxidant enzymes in maize leaves. J Exp Bot 53:2401–2410

Johanson U, Karlsson M, Johansson I, Gustavsson S, Sjövall S, Fraysse L, Weig AR, Kjellbom P (2001) The complete set of genes encoding major intrinsic proteins in Arabidopsis provides a framework for a new nomenclature for major intrinsic proteins in plants. Plant Physiol 126:1358–1369

Kawase M, Hanba YT, Katsuhara M (2013) The photosynthetic response of tobacco plants overexpressing ice plant aquaporin McMIPB to a soil water deficit and high vapor pressure deficit. J Plant Res 126:517–527

Klebl F, Wolf M, Sauer N (2003) A defect in the yeast plasma membrane urea transporter Dur3p is complemented by CpNIP1, a Nod26-like protein from zucchini (Cucurbita pepo L.), and by Arabidopsis thaliana δ-TIP or γ-TIP. FEBS Lett 547:69–74

Ligaba A, Katsuhara M, Shibasaka M, Djira G (2011) Abiotic stresses modulate expression of major intrinsic proteins in barley (Hordeum vulgare). C R Biol 334:127–139

Livak KJ, Schmittgen TD (2001) Analysis of relative gene expression data using real-time quantitative PCR and the $2^{-\Delta\Delta Ct}$ method. Methods 25:402–408

Ludevid D, Herman H, Edward H, Chrispeels aMJ (1992) The expression pattern of the tonoplast intrinsic protein γ-TIP in Arabidopsis thalianais correlated with cell enlargement. Plant Physiol 100(4):1633–1639

Luu DT, Maurel C (2005) Aquaporins in a challenging environment: molecular gears for adjusting plant water status. Plant Cell Environ 28:85–96

Möckli N, Deplazes A, Hassa P, Zhang Z, Peter M, Hottiger M, Stagljar I, Auerbach D (2007) Yeast split-ubiquitin-based cytosolic screening system to detect interactions between transcriptionally active proteins. Biotechniques 42:725–730

Ma DM, WR WX, Li HW, Jin FX, Guo LN, Wang J, Da HJ, Xu X (2014) Co-expression of the ArabidopsisSOS genes enhances salt tolerance in transgenic tall fescue (Festuca arundinacea Schreb.). Protoplasma 251:219–231

Ma JF, Yamaji N, Mitani N, Tamai K, Konishi S, Fujiwara T, Katsuhara M, Yano M (2007) An efflux transporter of silicon in rice. Nature 448:209–212

Ma S, Quist TM, Ulanov A, Joly R, Bohnert HJ (2004) Loss of TIP1; 1 aquaporin in Arabidopsis leads to cell and plant death. Plant J 40:845–859

Mahdieh M, Mostajeran A, Horie T, Katsuhara M (2008) Drought stress alters water relations and expression of PIP-type aquaporin genes in Nicotiana tabacum plants. Plant Cell Physiol 49:801–813

Maurel C (2007) Plant aquaporins: novel functions and regulation properties. FEBS Lett 581:2227–2236

Maurel C, Reizer J, Schroeder JI, Chrispeels MJ (1993) The vacuolar membrane protein gamma-TIP creates water specific channels in Xenopus oocytes. EMBO J 12:2241–2247

Maurel C, Tacnet F, Güclü J, Guern J, Ripoche P (1997) Purified vesicles of tobacco cell vacuolar and plasma membranes exhibit dramatically different water permeability and water channel activity. Proc Natl Acad Sci USA 94:7103–7108

Maurel C, Verdoucq L, Luu DT, Santoni V (2008) Plant aquaporins: membrane channels with multiple integrated functions. Annu Rev Plant Biol 59:595–624

Murozuka E, Hanisch S, Pomorski TG, Jahn TP, Schjoerring JK (2013) Bimolecular fluorescence complementation and interaction of various Arabidopsis major intrinsic proteins expressed in yeast. Physiol Plantarum 148:422–431

Niemietz CM, Tyerman SD (1997) Characterization of water channels in wheat root membrane vesicles. Plant Physiol 115:561–567

Obroucheva NV, Sin'kevich IA (2010) Aquaporins and cell growth. Russ J Plant Physiol 57:153–165

Otto B, Uehlein N, Sdorra S, Fischer M, Ayaz M, Belastegui-Macadam X, Heckwolf M, Lachnit M, Pede N, Priem N (2010) Aquaporin tetramer composition modifies the function of tobacco aquaporins. J Biol Chem 285:31253–31260

Park W, Scheffler BE, Bauer PJ, Campbell BT (2010) Identification of the family of aquaporin genes and their expression in upland cotton (Gossypium hirsutum L.). BMC Plant Biol 10:142

Polle A, Otter T, Seifert F (1994) Apoplastic peroxidases and lignification in needles of Norway spruce (Picea abies L.). Plant Physiol 106:53–60

Reuscher S, Akiyama M, Mori C, Aoki K, Shibata D, Shiratake K (2013) Genome-wide identification and expression analysis of aquaporins in tomato. PLoS One 8:e79052

Reyes F, Marchant L, Norambuena L, Nilo R, Silva H, Orellana A (2006) AtUTr1, a UDP-glucose/UDP-galactose transporter from Arabidopsis thaliana, is located in the endoplasmic reticulum and up-regulated by the unfolded protein response. J Biol Chem 281:9145–9151

Ruiz-Lozano JM, Porcel R, Azcón C, Aroca R (2012) Regulation by arbuscular mycorrhizae of the integrated physiological response to salinity in plants: new challenges in physiological and molecular studies. J Exp Bot 63:4033–4044

Sade N, Vinocur BJ, Diber A, Shatil A, Ronen G, Nissan H, Wallach R, Karchi H, Moshelion M (2009) Improving plant stress tolerance and yield production: is the tonoplast aquaporin SlTIP2;2 a key to isohydric to anisohydric conversion? New Phytol 181:651–661

Sakurai J, Ishikawa F, Yamaguchi T, Uemura M, Maeshima M (2005) Identification of 33 rice aquaporin genes and analysis of their expression and function. Plant Cell Physiol 46:1568–1577

Steven JC, Andrew FB (1998) Floral dip: a simplified method for *Agrobacterium*-mediated transformation of Arabidopsis thaliana. Plant J 16:735–743

Sun J, Chen S, Dai S, Wang R, Li N, Shen X, Zhou X, Lu C, Zheng X, Hu Z, Zhang Z, Song J, Xu Y (2009) NaCl-induced alternations of cellular and tissue ion fluxes in roots of salt-resistant and salt-sensitive poplar species. Plant Physiol 149:1141–1153

Takano J, Wada M, Ludewig U, Schaaf G, von Wirén N, Fujiwara T (2006) The *Arabidopsis* major intrinsic protein NIP5;1 is essential for efficient boron uptake and plant development under boron limitation. Plant Cell 18:1498–1509

Uno Y, Urano T, Yamaguchi-Shinozaki K, Kanechi M, Inagaki N, Maekawa S, Shinozaki K (1998) Early salt-stress effects on expression of genes for aquaporin homologues in the halophyte sea aster (*Aster tripolium* L). J Plant Res 111:411–419

Vera-Estrella R, Barkla BJ, Bohnert HJ, Pantoja O (2004) Novel regulation of aquaporins during osmotic stress. Plant Physiol 135:2318–2329

Verkman AS, Mitra AK (2000) Structure and function of aquaporin water channels. Am J Physiol Renal Physiol 278:13–18

Walter M, Chaban C, Schutze K, Batistic O, Weckermann K, Nake C, Blazevic D, Grefen C, Schumacher K, Oecking C, Harter K, Kudla J (2004) Visualization of protein interactions in living plant cells using bimolecular fluorescence complementation. Plant J 40:428–438

Yoo S-D, Cho Y-H, Sheen J (2007) *Arabidopsis* mesophyll protoplasts: a versatile cell system for transient gene expression analysis. Nature protocols 2:1565–1572

Zelazny E, Borst JW, Muylaert M, Batoko H, Hemminga MA, Chaumont F (2007) FRET imaging in living maize cells reveals that plasma membrane aquaporins interact to regulate their subcellular localization. Proc Natl Acad Sci USA 104:12359–12364